International Journal of Electrical and Computer Engineering (IJECE)
Vol. 6, No. 2, April 2016, pp. 583~595
ISSN: 2088-8708, DOI: 10.11591/ijece.v6i2.8809

Comparative Assessment on Linearity Test based V2π and Vπ/2 Voltage Variations of Closed Loop IFOG

T. Sireesha[1], K. Krishna Murthy[2]
[1]Department of ECE, Potti Sriramulu Chalavadi Mallikharjuna Rao College of Engineering and Technology, Vijayawada, Krishna (Dt), Andhra Pradesh, India
[2]Department of Electronics, P.G. Center, P.B. Siddhartha Arts & Science College, Vijayawada, Krishna (Dt), Andhra Pradesh, India.

Article Info

Article history:

Received Aug 14, 2015
Revised Nov 30, 2015
Accepted Dec 22, 2015

Keyword:

Biasing square wave signal
Voltage (Vπ/2)
Closed loop approach
Interferometric fiber optic
Gyroscope (IFOG)
Linearity
Ramp voltage (V2π)

ABSTRACT

Interferometric Fiber Optic Gyroscope (IFOG) has to operate in closed loop condition to achieve inertial grade performance. The closed loop system is mainly depends upon the amplitude of the ramp signal (V2π of IOC) and bias (square wave) signal frequency (f_{bias}). The digital phase ramp function is given as feedback to the optical system and makes gyro to null condition. The peak-to-peak amplitude (Vπ/2) of biasing signal is one-fourth of the ramp amplitude (V2π). If there are any variations in the amplitude of the ramp and biasing signals, then it introduces variations in the gyro performance. In this paper, a comparative discussion made in the gyro parameters for three cases: (i) V2π (vary) & Vπ/2 (constant), (ii) Vπ/2 (vary) & V2π (constant) and (iii) both V2π and Vπ/2 are varying simultaneously. The effects on gyroscope are described with the derived values in terms of linearity. From the experimental results, it was observed that the gyro output is very sensitive with respect to V2π variations and obtained the percentage error of 10% in gyro output, but very less effect due to Vπ/2 variations. So, the proper resetting of ramp voltage (V2π) is required to avoid nonlinearities and instabilities in gyro output.

Corresponding Author:

T. Sireesha,
Assistant Professor, Department of ECE,
Potti Sriramulu Chalavadi Mallikharjuna Rao College of Engineering and Technology,
Vijayawada, Krishna (Dt), Andhra Pradesh, India.
Email: sirishatammana@ rediffmail.com

1. INTRODUCTION

A fiber optic gyroscope (FOG) senses changes in orientation, thus performing the function of a mechanical gyroscope. FOG is an important development in the field of fibre optic sensors, which have been studied and developed more than two decades. FOGs are used in Inertial Navigation System (INS), guidance, control systems in aircraft and spacecraft etc.

FOGs are designed to measure the rotation induces path difference as measure of phase or frequency difference between the counter propagating waves. Two different configurations exist: Interferometric Fiber Optic Gyroscope (IFOG) and Resonant Fiber Optic Gyroscopes (RFOG). The induced optical path difference can be measured in two ways (i) by measuring a frequency in a laser resonator or in a resonator fibre optic gyroscope (ii) by measuring a phase of two interfering beams in an Interferometric fiber optic gyroscope [1]. The RFOG is used in research stages and performance of the gyroscope is limited by backscattering noise of frequency [2]. A better alternative to traditional spinning mass gyroscopes proven by IFOGs, have high reliability, wide dynamic range, low power consumption, light weight, and low cost [3].

The signal processing scheme of a IFOG is broadly classified into two major categories namely an open loop approach and a closed loop approach, but restricts it presently in Avionics and Inertial Navigation

Grade applications [4] due to its complexity of the former. In open loop IFOG system the rotation rate sensing is obtained through a direct measurement [5], but this system is not perfectly stable because there is a variation in the returning optical power, changes in the amplitude of the phase modulation in the demodulated biased signals which will cause errors in detector output and the response is nonlinear, limited dynamic range, low accuracy and less sensitivity.

In order to eliminate the dependency of the light intensity a closed loop scheme is used. In closed loop IFOG system the rotation rate sensing is obtained through a feedback (ramp) signal to nullify the rotation-induced Sagnac phase error. The analog solution of closed loop configuration, based on an analog phase ramp with a biasing (sine wave) modulation, does not represent a very efficient solution because the output is very sensitive to the environment. A great improvement is achieved with the digital closed-loop configuration of biasing (square wave) modulation and feedback phase ramp is adopted to suppress the closed loop error near the zero point and to improve the linear characteristic and stabilize the scale factor and its insensitiveness against environment, especially against vibration. However, the closed loop IFOG system is stable and has good accuracy [6].

2. DESRIPTION OF FIBER OPTIC GYROSCOPE

Fiber optic gyroscope is a rotation sensor, working on the principle of sagnac effect. Sagnac first demonstrated the optical gyroscope principle in 1913. Implementation of optical gyroscopes was done by using Sagnac effect, so far, which states that induced optical path difference by counter propagating beams in a rotating reference frame is proportional to the absolute rotation [7], [8]. The operation principle of Sagnac interferometer is as shown in Figure 1.

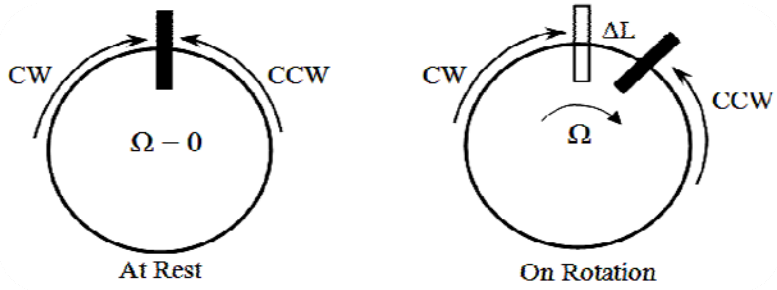

Figure 1. Sagnac Interferometer Working Principle

When system has no rotation (i.e., at rest) the light propagating in clockwise (CW) and counter clockwise (CCW) directions traverse identical paths, then there is no phase difference between them. When the system rotates at an angular rotation rate Ω, then the beam of light rotating with ring has optical path longer then the counter propagating beam by a distance $\frac{LR}{C}\Omega$ [5]. The resultant rotation induced sagnac phase shift is,

$$\Delta\phi_s = \frac{2\pi LD}{\lambda C}\Omega \quad (1)$$

Where, D is diameter of the sensor coil, L is length of the optical fiber, λ is light wavelength, Ω is rotation rate and C is speed of light in vacuum [1], [9].

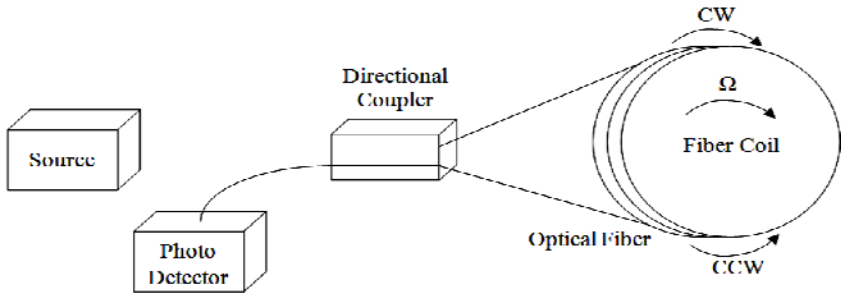

Figure 2. Basic Configuration of FOG

A basic FOG configuration is shown in Figure 2. In two-wave interferometer, the intensity on the photo detector represents with a combination of the two light waves, varies as cosine of Sagnac phase with its maximum value at zero.

This intensity (I or I_d) is expressed as,

$$I_d = I_0(1+\cos(\Delta\phi_s)) \quad (2)$$

Where, I_0 is the mean value of the intensity. The rotation rate is calculated with the detected intensity [6].

The limitations in the basic configuration are [7], [10]: Poor sensitivity for small rotation rates, direction ambiguity, restricted dynamic range due to the 2π periodicity of the response curve and output is a nonlinear function of the rotation rate. The problems of poor sensitivity and direction ambiguity are usually overcome by the application of the differential phase modulation.

2.1. The Open Loop Configuration

A phase modulator is used for this purpose and it is placed in asymmetric position in the sensing fiber loop, so that two counter propagating waves pass through the modulator at different time instants before that interfere with each other than different phase delay is obtained by counter propagating waves [11], [12].

In open loop approach, a lock in amplifier is used to measure the photo detector output at the fundamental mode frequency and the rotate rate is directly computed from this measurement [13], [14]. Additionally, the amplitude of the second and higher harmonics may also be measured to compensate for the variations in the returning optical power and changes in the amplitude of different phase modulation [15]. The block diagram of an open loop FOG is as shown in Figure 3 [13].

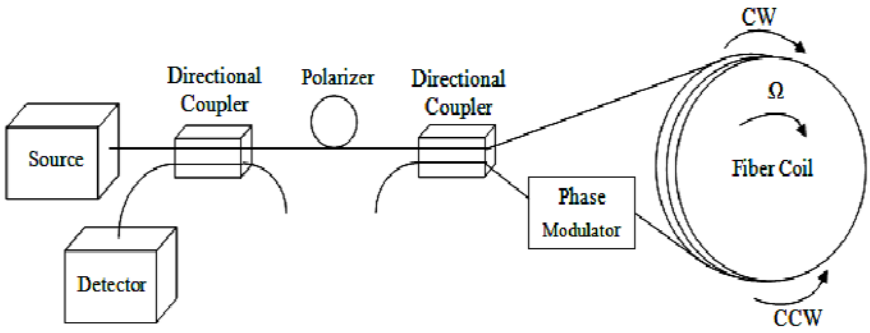

Figure 3. Open Loop Configuration Fiber Optic Gyroscope with Phase Modulator.

This creates phase difference between two counter propagating beams. When a phase modulator is used, the expression for the intensity on the photo detector is,

$$I_d = I_0(1+\cos((\Delta\phi_s)+\Delta\phi_m)) \quad (3)$$

Even though, there is a drawback exists in open loop approach due to variations in the returning optical power and changes in the amplitude of the phase modulation which will cause errors in output [7], [10] and the response is nonlinear, limited dynamic range, low accuracy and less sensitivity.

2.2. The Closed Loop Configuration

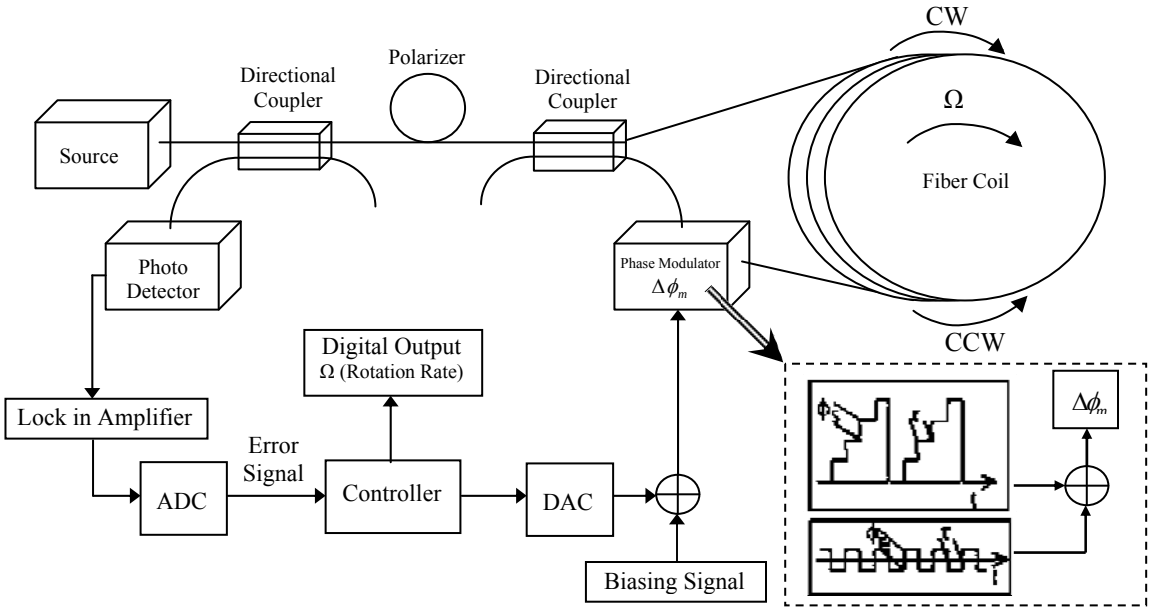

Figure 4. Schematic diagram of closed loop fiber optic gyroscope with digital phase ramp function

In closed loop approach, the photo detector output demodulated at the phase modulation frequency is used as an error signal. This loop introduces a controlled amount of non reciprocal phase difference between the two counter propagating optical waves to counteract the rotation induced signal phase shift [15], [16]. The block diagram of closed loop FOG is shown in Figure 4.

Thus the net phase difference between the two interfering waves is maintained at zero regardless of the rotate rate. It introduces the amount of nonreciprocal phase shift is the output of the gyroscope and is linearly with respect to rotate rate [7], [10], [16] i.e., it is fed back into the system to generate an feedback phase difference ϕ_{fb} that is maintained opposite to the Sagnac phase shift $\Delta\phi_s$

$$\text{Therefore,} \quad \phi_{fb} = -\Delta\phi_s \tag{4}$$

The advantages of the closed loop system [17] are: No moving parts, High Linearity, Wide dynamic range, Very rugged, Good Accuracy and High sensibility, Bias stability, Scale Factor linearity and stability, long and reliable lifetime and Low cost [18].

3. HARDWARE AND SOFTWARE INTERFACE

The proposed approach is to generate the feedback signal for compensating the phase error of CLFOG as shown in the Figure 5. Here, the feedback loop is made by different components such as Signal conditioning Amplifier (SCA), ADC, FPGA, DAC, temperature sensor and output differential driver CLFOG is biased with square wave signal of period equal to transit time (τ) of the fiber-coil. Here, a square wave modulation is used to modulate the light, thereby to increase the sensitivity and to detect the rotation rate polarity. The PINFET converts optical power, which is output of FOG to electrical signal. This output is square wave modulated co-sinusoidal signal. The system accepts modulated Sagnac Phase error data is received through PINFET output of CLFOG. On-board 16-bit ADC will receive the data from PINFET and will be processed by using FPGA. It is demodulated to extract the Sagnac phase error and used to generate the feedback signal for the phase modulator is given through 16-bit DAC. This feedback signal represents phase-error-compensation signal to achieve closed loop functionality of the system [19], [20].

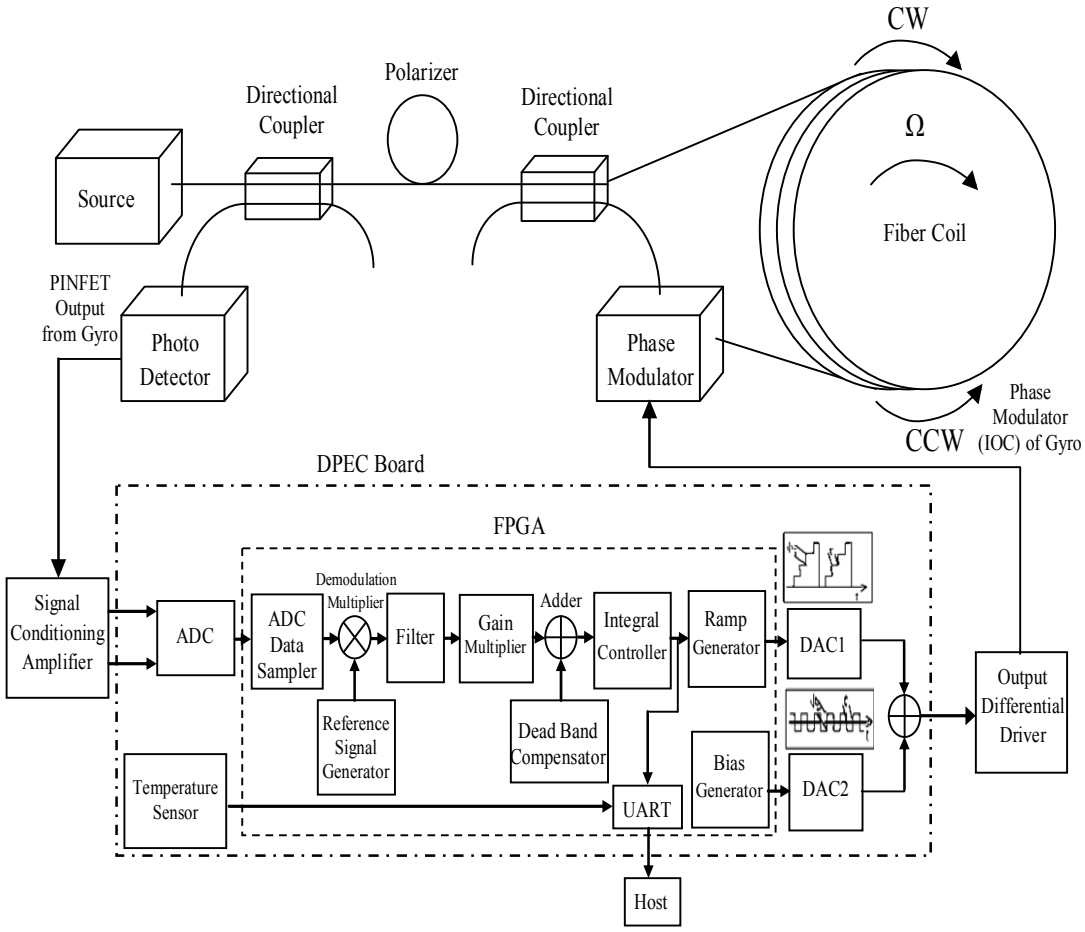

Figure 5. Proposed Design Approach of CLFOG

The feedback phase nullifying signal (ramp signal voltage is V2π and its frequency 200 KHz) and the biasing signal (square wave signal voltage is Vπ/2 and its frequency of 100 KHz) are used as control signals for CLFOG. So the ramp and the square wave biasing signal for the phase modulator (IOC) of the FOG are given through 16-bit DAC. The DPEC board transfers the phase integrator output to the host by compensating the temperature induced bias errors, upon the request of synchronization pulses [21]. In the current design, with a selected time of every 2ms the averaged step-size data is sent via UART to the PC.

3.1. Hardware Interface

The hardware implementation of CLFOG system (as shown in Figure 5), some of the components are discussed below:

1) FPGA

FPGA is used in interfacing with various components, performing digital signal processing functions and communicating with user interface.

2) ADC Interface

It is a 16-bit parallel interface used to receive data from ADC to FPGA. This data represents the modulated gyro phase error. Clock and reset to ADC is driven by FPGA. Data read synchronization control is driven by FPGA. Maximum sampling rate of ADC is 4MHz.

3) DAC1 and DAC2 Interface

It is also a 16-bit parallel interface used to provide data from FPGA to DAC1 and DAC2. This DAC1 data represents the square wave bias signal used for intensity modulation, whereas the DAC2 data represents the phase error compensating signal and the nature of this compensating signal is stair case ramp. Clock signal to DAC is driven by FPGA. Maximum sampling rate of DAC is 20MHz.

4) RS232/RS422 Interface

This interface is used for Communicating with PC application software, which was implemented on UART. FPGA acting as Master of communication transfers the desired data to PC. Configuration parameters from PC are received on the serial line.

5) Temperature Sensor (AD7415) Interface

AD7415 is an I2C based 10-bit temperature sensor is used to collect temperature data on this interface (both On-board sensor and other connectors).

3.2. Software Interface

In software Implementation of CLFOG system, to measure the rotation rate in fiber optic gyroscope, we require some software's as follows: ProAXE SE 5.5.0, Real term serial capture program, Dev C++, Matlab program, XILINX ISE 10.1. However, the ProAXE SE software is a GUI Interface used to control the rate table operation of gyro. It is used for testing process given to our experimental setup operated in two modes (i.e., manual and automatic modes) whereas, the Real term serial capture program software is used to capture the data (hex values) from FOG and it is given to host through a MOXA Uport serial adapter.

4. TEST PROCEDURE

The FOG is subjected to various kinds of tests to certain its performance in terms of linearity. The gyro has externally available terminals for temperature sensor readout for each test and it is noted that all tests require stable temperatures to perform at thermal equilibrium. The gyro operating temperature is taken from 25°C to 40 °C.

Before going to the testing procedure and after switch ON the power supply, check whether the Gyro output (PINFET), biasing (square wave) and ramp signals outputs in the equipment are getting properly or not.

The proper fine tuning of the closed loop approach was observed by doing the process implementation as shown in Figure 6. The gyro requires more than one input voltage. For each circuit, operating voltage and current should be specified in order to measure and record the input power required from each source.

Before starting up the test process, mount the gyro (CLFOG) in the fixture on the rate table so that the input reference axis (z-axis) is parallel to the table rotational axis, as shown in the Figure 7 test setup. Connect the gyro to the output measuring and recording equipment (software in PC). Apply power to the gyro and record the gyro output with respect to time. Here, the gyro output consists of raw data and the average data for corresponding rate against temperature

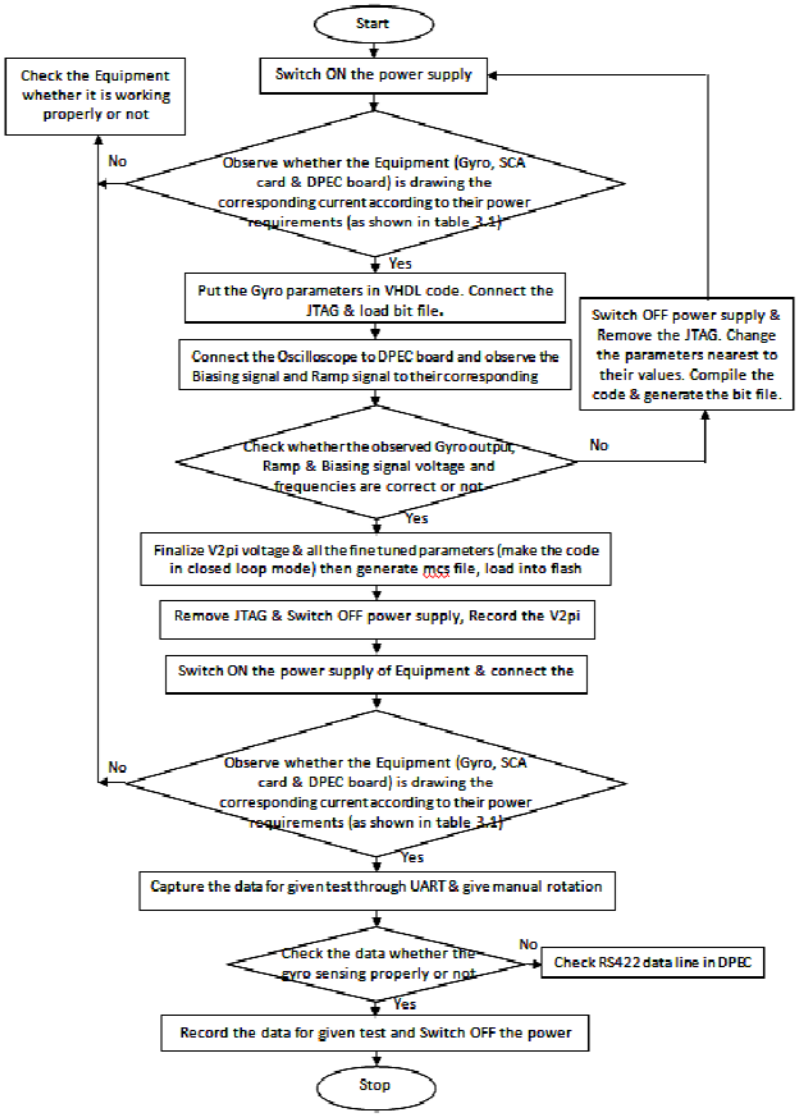

Figure 6. Process Implementation for Fine Tuning of the Closed Loop Approach

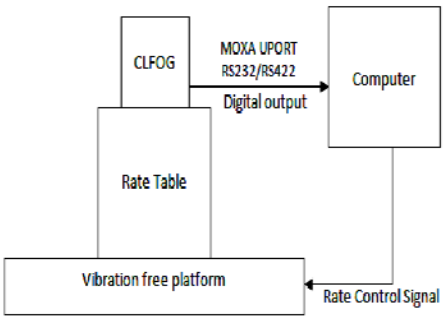

Figure 7. Test Setup

5. RESULTS AND COMPARISONS

In the testing results, first open-loop and closed-loop configurations are demonstrated with rotations.

5.1. The Open Loop Configuration

The output of the open loop configuration with rotation was observed in the oscilloscope as shown in the Figure 8. In this figure the first waveform represents the gyro output, the second represents the ramp signal and the third represents the square-wave biasing signal. In the open-loop, the amplitude of the gyro output changes with the rotation according to the square-wave biasing signal but included with the error. The ramp remains constant even with the rotation.

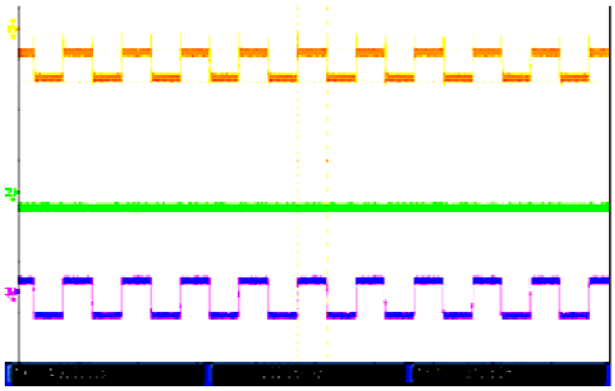

Figure 8. Output of the open loop configuration with rotation

5.2. The Closed Loop Configuration

The output of the closed loop configuration with rotation was observed in the oscilloscope as shown in the Figure 9 (a). The feedback loop is not closed properly, so the output is changed at reset of the ramp. To remove this error, the amplitude of the ramp voltage is adjusted to 8.75V with a frequency of 200 KHz. The gain is adjusted to compensate the error in the amplitude of the gyro output. The biasing signal is also changed according to the ramp voltage. After adjusting the amplitude of the ramp voltage, the output of closed loop configuration of proper fine tuning with rotation was observed in the oscilloscope as shown in the Figure 9 (b).

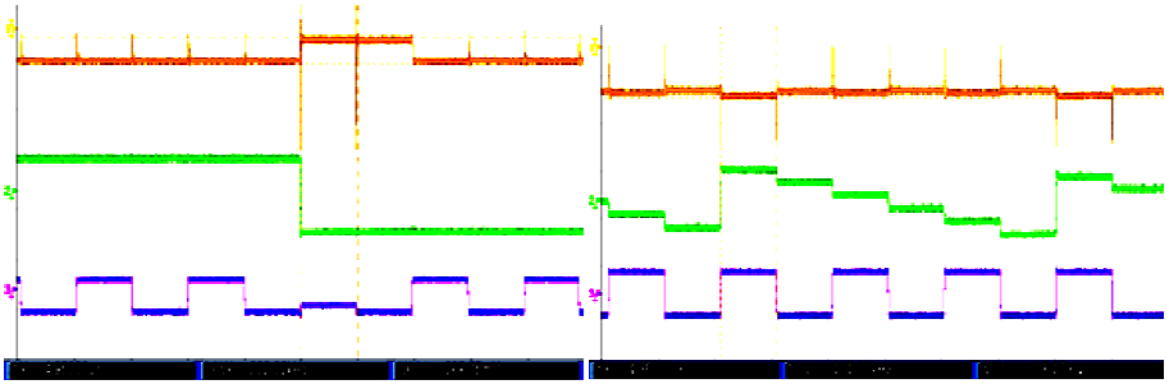

(a) (b)

Figure 9. Output of closed loop configuration (a) without fine tuning (b) with fine tuning

After fine tuning, the Gyro output (PINFET), biasing (square wave) and ramp signals outputs in the DPEC board are observed in the oscilloscope is as shown in Figure's 10, 11 & 12.

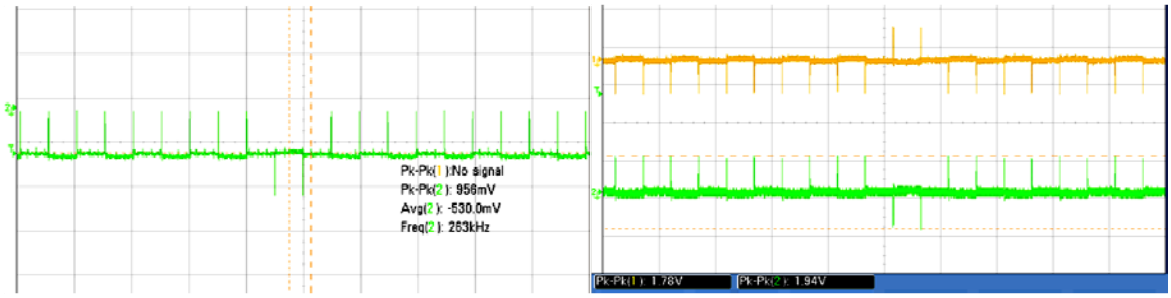

(a) (b)

Figure 10. (a) PINFET output and (b) Differential PINFET output of a SCA amplifier before ADC

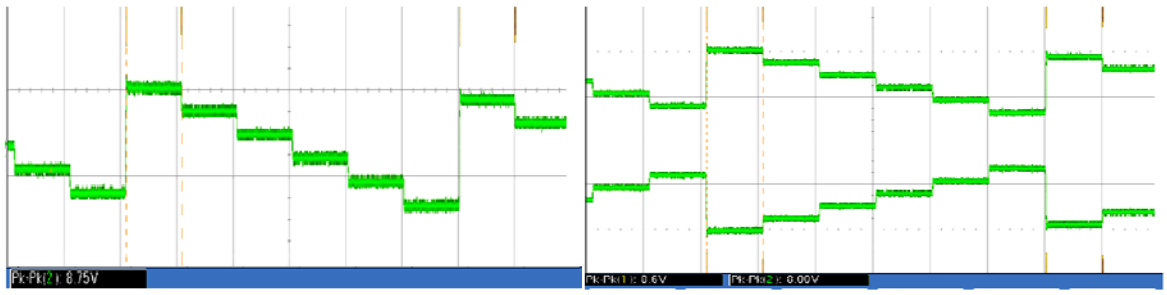

(a) (b)

Figure 11. (a) Ramp Signal output at DAC 1 and (b) Differential Ramp Signal output at driver 1

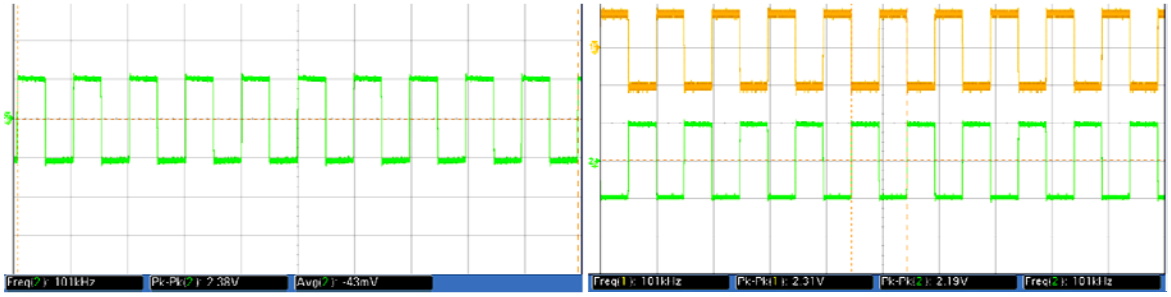

(a) (b)

Figure 12. (a) Bias Signal (square wave) output at DAC 2 and (b) Differential Bias Signal output at driver 2

5.3. Test Results

The linearity test was performed and its result (proper fine tuning of closed loop gyro when V2π=8.75V) in MATLAB as shown in Figure 13 and the test results describe the linearity response of our proposed closed loop gyro system [22], [23]. The ramp voltage (or bias voltage) is increased from 1% to 10% and decreased to 1% to 10% and performed the various tests in the below three cases:

Case 1: V2π (ramp signal voltage) is varied and Vπ/2(square wave biasing signal voltage) is fixed.
Case 2: Vπ/2 (square wave biasing signal voltage) is varied and the fine tuned voltage V2πis fixed.
Case 3: Both V2π (ramp signal voltage) and Vπ/2 (square wave biasing signal voltage) are varied simultaneously.

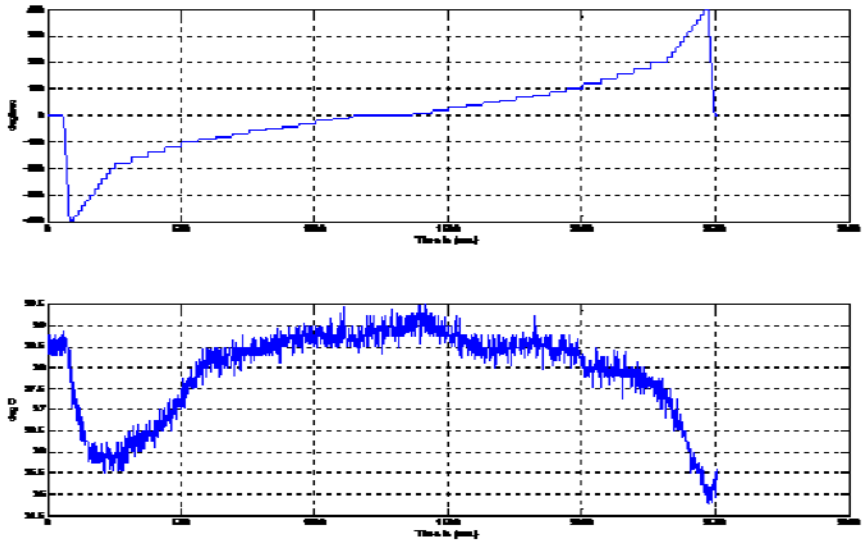

Figure 13. Linearity Test of the Gyro Output against temperature for closed loop with proper fine tuning

The linearity test waveforms for each test and their tabulation are as shown below. The linearity test is performed for 42 minutes for each case within a dynamic range of - 400 deg/sec to + 400 deg/sec. In three cases, comparison is made in terms of its linearity and it is tabulated as shown in the table-1 (a, b & c) and recorded the corresponding maximum and minimum nonlinearities for three cases.

Table 1. Comparison of linearity for three cases

(a)

%	Max. Non-Linearity	Min. Non-Linearity
-10%	74401.82	-54742.36
-9%	79215.30	-44836.56
-8%	34312.72	-29535.00
-7%	18304.01	-22702.47
-6%	5854.40	-18803.00
-5%	1317.00	-7440.80
-4%	1537.90	-1986.40
-3%	2331.90	-989.33
-2%	4277.80	-4844.30
-1%	1570.40	-2457.30
--	1313.60	-1290.10
1%	7949.70	-12441.00
2%	7673.16	-2007.70
3%	6355.00	-6229.60
4%	7695.30	-1595.00
5%	12834.00	-1802.90
6%	16532.00	-8478.10
7%	16374.00	-23949.00
8%	20400.00	-14813.00
9%	25084.00	-12932.00
10%	36366.00	-15803.00

(b)

%	Max. Non-Linearity	Min. Non-Linearity
-10%	2688.50	-3126.10
-9%	684.21	-2050.50
-8%	596.31	-2587.10
-7%	1136.00	-1970.60
-6%	2700.00	-3482.00
-5%	892.66	-2517.70
-4%	956.70	-2371.20
-3%	1134.40	-1916.20
-2%	1640.80	-1978.40
-1%	1325.50	-1638.50
--	1313.60	-1290.10
1%	905.97	-927.39
2%	1835.20	-852.05
3%	1112.10	-618.84
4%	2028.30	-1052.50
5%	715.85	-320.57
6%	2345.50	-947.60
7%	1313.70	-565.32
8%	1298.80	-917.00
9%	3696.70	-1287.50
10%	1837.40	-397.62

(c)

%	Max. Non-Linearity	Min. Non-Linearity
-6%	8095400.00	-2419100.00
-5%	342300.00	-2446000.00
-4%	37126.00	-48338.00
-3%	19309.00	-35850.00
-2%	1755.50	-5697.40
-1%	2653.20	-3393.00
--	1313.60	-1290.10
1%	928.99	-1653.80
2%	887.67	-3833.20
3%	1706.20	-4748.40
4%	4316.70	-3456.70
5%	16583.00	-4109.80
6%	11772.00	-1767.20
7%	106490.00	-4268.10
8%	11416.00	-4554.10
9%	17792.00	-5367.50
10%	37662.00	-13060.00

Then the actual output rotation rate was observed for a given input rotation rate for three cases as shown in the Figure 14 (a, b & c).

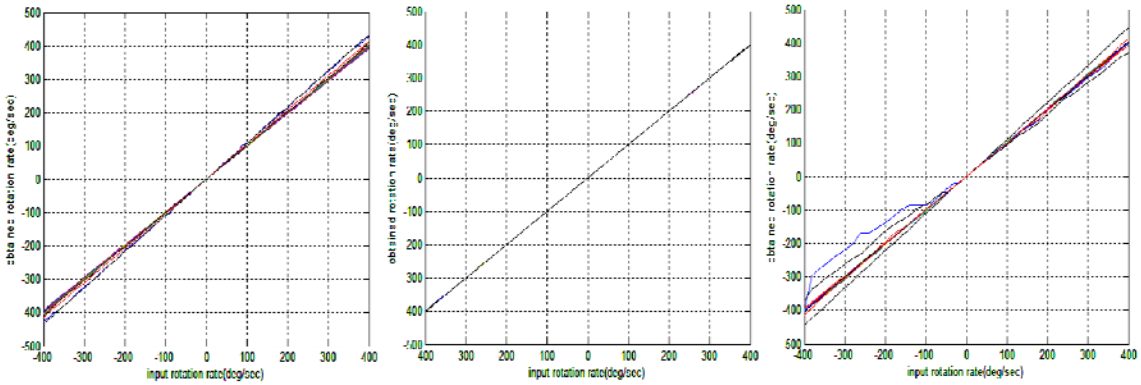

(a) (b) (c)

Figure 14. Comparison of linearity for three cases

The percentage error was also observed for each case, corresponding to given rotation rate when the ramp voltage is increased from 1% to 10% and decreased to 1% to 10% shown in Figure's 15 (a, b & c) and 16 (a, b & c).

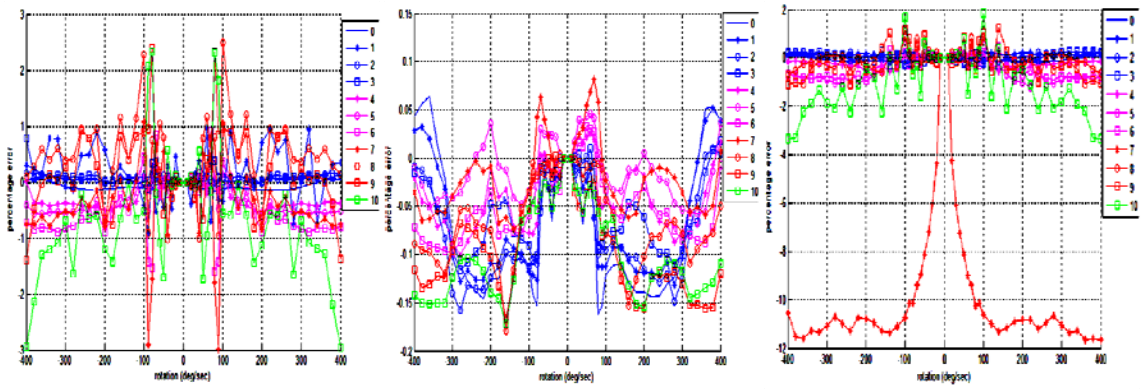

(a) (b) (c)

Figure 15. Comparison of percentage error when increased from 1% to 10% for three cases

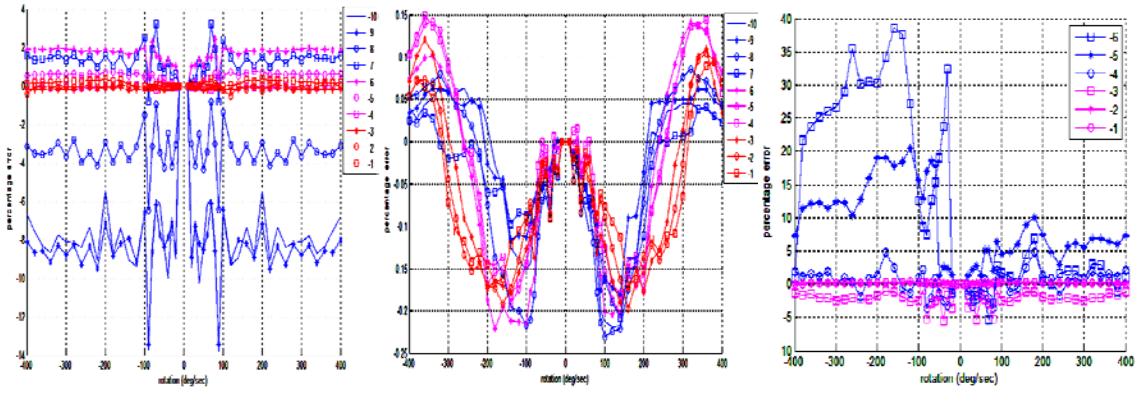

(a) (b) (c)

Figure 16. Comparison of percentage error when increased from 1% to 10% for three cases

6. CONCLUSION

In this paper, our proposed (digital) approach was to derive the rotation rate in closed loop IFOG system is investigated theoretically and experimentally. The performance of gyroscope was studied and the comparisons for variations in gyro parameters are made for three cases ((i) V2π (vary) & Vπ/2 (constant), (ii) Vπ/2 (vary) & V2π (constant), and (iii) both V2π & Vπ/2 are varied). From the experimental results, it was observed as follows:

(i) When ramp voltage (V2π) is varying and square-wave voltage (Vπ/2) is kept constant, then the output is not maintaining the linearity and the percentage error is high.

(ii) When ramp voltage (V2π) is kept constant and biasing signal voltage (Vπ/2) is varying, the effect is very minute. The percentage error is too low.

(iii) When both ramp and square-wave voltage is simultaneously changed, then it was observed that the device is not responding accordingly as the error is increasing. The rotations are not sensed properly.

All these experimental results are therefore compared with the values derived in terms of linearity. Finally, concluded that the gyro performance is very sensitive with respect to ramp voltage (V2π) variations and obtained the percentage error of 10% in gyro output, but very less effect due to biasing signal voltage (Vπ/2) variations when the ramp voltage is constant. In order to avoid the nonlinearities and instabilities, a proper resetting of the ramp voltage (V2π) is required.

ACKNOWLEDGEMENTS

The author T.Sireesha would like to express her sense of gratitude to Dr. Jagannath Nayak (SC-G), Director and G. Krishna Prasad (SC-D), Department of Inertial Systems Group, Research Center Imarat - RCI, Hyderabad, INDIA, is great-fully acknowledged for their valuable guidance and constant review in connection to completion of this project work and also express my thanks to the management of RCI for their support and encouragement during this work. Further, it gives me immense pleasure to thank my guide Dr. K. Krishna Murthy PG-Director, P.B. Siddhartha college of arts and science, for their cooperation and help with the data collection in connection to this work.

REFERENCES

[1] Jagannath Nayak. Fiber-Optic Gyroscopes: from design to production. *Applied Optics*, 2011; 50(25); E152-E161.
[2] Mohammad Reza Nasiri Avanaki, et al. Comparative Assessment on the Performance of Open-Loop and Closed-Loop IFOGS. Electronic Engg Department, Azad University of Karaj, Tehran, Iran and RAZI University, Kermanshah, Iran, *Optics and Photonics Journal*, March 2012; 2(1), 17-29.
[3] Ashley Paul R., et al. *Test and Measurement Applications of Optoelectronic Devices.* 2002.
[4] S.M. Bennett, et al., Fiber Optic Gyroscope for Vehicular Use. AndrewCorpooration, Orland Park, IL, USA, *IEEE Jour. Light. Tach, vol 0-7803-4269-0, IEEE Standards,* 1998; Boston, MA, 1053-1057.
[5] Mr. Avanaki. *Full Progress of Digital Signal Processing in Open Loop-IFOG.* Asian Optical Fiber Communication & Optoelectronic Exposition & Conference, 10/2006.
[6] Ruffin Paul. *Fiber Optic Gyroscope Sensors.* Optical Science and Engineering, 2008.
[7] G. Krishna Prasad and Jagannath Nayak. *Design, Fabrication and Testing of Digital Signal Processing Scheme for Inertial Grade Fiber Optic Gyroscope* (FOG). Inertial System Group, Research Center Imarath, RCI, Hyderabad, 2011, 10 pages.
[8] Chunduru Vardhani, et al. *Integrated Optics Devices Materials and Technologies*. XIV, 2010.
[9] Sabina Merlo, et al. Fiber Gyroscope Principles. Electro optics Group, University of Pavia, Italy, *Handbook of Fibre Optic Sensing Technology,* edited by José Miguel López-Higuera, ISBN-X-XXX-XXXXX-X 2000; John Wiley & Sons Ltd, 1-23.
[10] Radha Madhuri Rajulapati and Jagannath Nayak. *Modeling and Simulation of Signal Processing for a Closedloop Fiber Optic Gyro's using* FPGA", Dept of ECE, K.L.University,Vijayawada, Andhra Pradesh, and Scientist – RCI, Hyderabad, 2012; 4(3); 947-959.
[11] Feng Sun, et al. Study on the drift of Modulated Phase Ininterference Fiber Optic Gyroscope. Harbin Engineering University, Harbin, China, *Journal of Computers*, March 2010; 5(3); 394-400.
[12] B.Y. Kim and H.J. Shaw. *Fiber Optic Gyroscope Principles.*
[13] I.M.H. Khan, et al. Open-Loop Fiber-Optic Gyroscope - A Technical Note. Hindustan Aeronautics Limited. Korwa, and Institute of Armament Technology, Pune - 411 025, *Defence Science Journal,* October 1996; 46(4); DESIDOC; 283-288.
[14] Medjadba H. *An optimal Open-Loop Multimode Fiber Gyroscope for Rate-Grade Performance Applications",* Optical Fiber Technology, 2011/12.
[15] Celikel, O¿uz, and S. Eren San. Establishment of all Digital Closed-Loop Interferometric Fiber Optic Gyroscope and Scale Factor Comparison for Open-Loop and all Digital Closed-Loop Configurations. *IEEE Sensors Journal,* 2009.

[16] Q.D. Sun, et al. "FPGA based Hardware Design of Closed Loop Control for Fiber Optic Gyroscope", Assoc. Prof., School of E&E Engineering, Shanghai Second Polytechnic University, Shanghai, and Dept of Earth and Space Science and Engineering, York University, Toronto, ON, Canada, *Journal of Theoretical and Applied Information* Technology, 10th May 2013; 51(1); JATIT & LLS; 121-128.
[17] Byoungho Lee. Review of the Present Status of Optical Fiber Sensors. School of Electrical Engineering, Seoul National University, Kwanak-GuShinlim-Dong, Seoul 151-744, South Korea, *Elsevier Science (USA),* 2003; 9(2); 57-79.
[18] Li. Xuyou. *Application of adaptive filtering to Digital Closed-Loop Fiber Optic Gyroscope.* International Conference on Mechatronics and Automation, 08/2009.
[19] Xiangjun Li. *Modeling and Simulation of Digital Closed-Loop Fiber Optic Gyroscope.* 6TH World Congress on Intelligent Control and Automation, 2006.
[20] Seçmen, Başak and Serhat Çakır. *Simulation on Interferometric Fiber Optic Gyroscope with Amplified Optical Feedback.* Department of Physics Supervisor, September 2003; 87 Pages.
[21] Gu Hong, et al. Real-Time Dynamic Simulation of angular velocity and suppression of dead zone in IFOG. *Optical Review,* 2015; 22(1); 39-45.
[22] Vladimir Vukmirica. *Interferometric* Fiber Optic Gyroscope: principle of operation and basic parameters determination", MSc (Eng), UDK: 629.1.054:629.052, COSATI: 17-07, *Scientific Technical Review,* Vol. LVIII, No.3-4, 2008; 83-91.
[23] Hui Li, et al. *Analysis and optimization of dynamic measurement precision of Fiber Optic Gyroscope.* School of Instrument Science and Optoelectronics Engineering, Beihang University, Beijing, China, 2013; Article ID 265895; 9 pages.
[24] Zhou Shiqin, et al. *Fiber Optic Gyros. 20th Anniversary Conference,* 1996.

BIOGRAPHIES OF AUTHORS

T. Sireesha is currently working as an Assistant Professor in the Department of Electronics and Communication Engineering, Potti Sriramulu Chalavadi Mallikharjuna Rao College of Engineering and Technology, Vijayawada and the research Scholar from the Department of Electronics at Acharya Nagarjuna University, Guntur. She has published 5 papers in the various research areas of Fiber Optics Communication and Sensor Technology, Signal Processing and Embedded Systems.

Dr. K. Krishna Murthy is a Director and Head of Department of Physics & Electronics, P.G. Center, P.B. Siddhartha Arts & Science College, Vijayawada, Krishna (Dt), Andhra Pradesh, India. He has more than 20 years of experience in his teaching profession. His research areas are in Physics and Electronics, Fiber Optics Communication and Sensor Technology.